

Endothelial basement membrane laminin $\alpha 5$ selectively inhibits T lymphocyte extravasation into the brain

Chuan Wu¹, Fredrik Ivars², Per Anderson^{2,9}, Rupert Hallmann¹, Dietmar Vestweber³, Per Nilsson⁴, Horst Robenek⁵, Karl Tryggvason⁶, Jian Song¹, Eva Korpos¹, Karin Loser⁷, Stefan Beissert⁷, Elisabeth Georges-Labouesse⁸ & Lydia M Sorokin¹

Specific inhibition of the entry of encephalitogenic T lymphocytes into the central nervous system in multiple sclerosis would provide a means of inhibiting disease without compromising innate immune responses. We show here that targeting lymphocyte interactions with endothelial basement membrane laminins provides such a possibility. In mouse experimental autoimmune encephalomyelitis, T lymphocyte extravasation correlates with sites expressing laminin $\alpha 4$ and small amounts of laminin $\alpha 5$. In mice lacking laminin $\alpha 4$, laminin $\alpha 5$ is ubiquitously expressed along the vascular tree, resulting in marked and selective reduction of T lymphocyte infiltration into the brain and reduced disease susceptibility and severity. Vessel phenotype and immune response were not affected in these mice. Rather, laminin $\alpha 5$ directly inhibited integrin $\alpha 6\beta 1$ -mediated migration of T lymphocytes through laminin $\alpha 4$. The data indicate that T lymphocytes use mechanisms distinct from other immune cells to penetrate the endothelial basement membrane barrier, permitting specific targeting of this immune cell population.

During leukocyte extravasation into inflamed tissues, cells quickly traverse the endothelial cell monolayer where they subsequently face the endothelial basement membrane. Previous data has shown that although leukocyte transmigration of the endothelial cell monolayer occurs within 2–5 min, penetration of the underlying basement membrane requires 20–30 min, indicating that the latter is a key rate-limiting step^{1–4}. However, the contribution of the basement membrane to endothelial barrier function remains uninvestigated owing to difficulties in studying this structure in a physiologically relevant manner.

Vascular basement membranes are complex assemblies of four glycoprotein families—laminins, collagen type IV, nidogens and heparan sulfate proteoglycans—that cannot be isolated as an intact structure or reconstituted *in vitro*. Although some basement membrane components can be purified in amounts that permit *in vitro* testing for their ability to support leukocyte adhesion and migration, barrier function cannot be studied, as the isolated molecules lack the complex molecular interactions that constitute basement membranes. Furthermore, the isoform composition of the four major basement membrane components varies with tissue type, and variations in their proportions may influence direct and indirect interactions within the network⁵.

The most physiologically relevant studies of basement membrane contribution to leukocyte extravasation use *in vivo* inflammatory models^{3,6–8} or intravital approaches^{9,10}. Experimental autoimmune

encephalomyelitis (EAE), a CD4⁺ T lymphocyte-mediated autoimmune disease with relevance to the human disease multiple sclerosis, has the advantage that, owing to the specialized structure of central nervous system (CNS) blood vessels, sites of extravasating leukocytes can be unequivocally identified. Extravasation occurs across postcapillary venules where, apart from the endothelial cell monolayer and underlying basement membrane, vessels are ensheathed by a second basement membrane, the parenchymal basement membrane, produced by astrocytes and leptomeningeal cells^{7,8,11}. In the course of EAE, leukocytes accumulate in the perivascular space between the endothelial and parenchymal basement membranes, leading to easily identifiable perivascular cuffs. Leukocytes use different mechanisms to penetrate endothelial and parenchymal basement membranes, with the latter requiring focal matrix metalloproteinase (MMP-2 and MMP-9) activity^{8,12}. Leukocyte penetration of the endothelial cell monolayer and its basement membrane is MMP-2 and MMP-9 independent⁸ and unique in several aspects. Intravital fluorescence videomicroscopy has revealed an integrin $\alpha 4$ - and P-selectin-dependent rolling of leukocytes along CNS vessels, without the involvement of E-selectin as in other tissues¹³, and an integrin $\alpha 4\beta 1$ -mediated, G protein-independent capture of T cells at the endothelial cell surface^{14,15}. Further, functional expression of lymphoid chemokines (CC chemokine ligand-19 (CCL19) and CCL21) rather than inflammatory chemokines occurs in CNS venules

¹Institute for Physiological Chemistry and Pathobiochemistry, Münster University, Münster, Germany. ²Section for Immunology, Department of Experimental Medical Science, Lund University, Lund, Sweden. ³Max Planck Institute for Molecular Biomedicine, Vascular Cell Biology, Münster, Germany. ⁴Radiation Physics, Lund University, Lund, Sweden. ⁵Leibniz Institute for Arteriosclerosis Research, Münster University, Münster, Germany. ⁶Department of Medical Biochemistry and Biophysics, Karolinska Institute, Stockholm, Sweden. ⁷Department of Dermatology, Münster University, Münster, Germany. ⁸Institut de Génétique et de Biologie Moléculaire et Cellulaire, Strasbourg, France. ⁹Current address: Instituto de Parasitología y Biomedicina, Parque Tecnológico de Ciencias de la Salud, Armilla (Granada), Spain. Correspondence should be addressed to L.M.S. (sorokin@uni-muenster.de).

Received 30 October 2008; accepted 1 April 2009; published online 26 April 2009; doi:10.1038/nm.1957

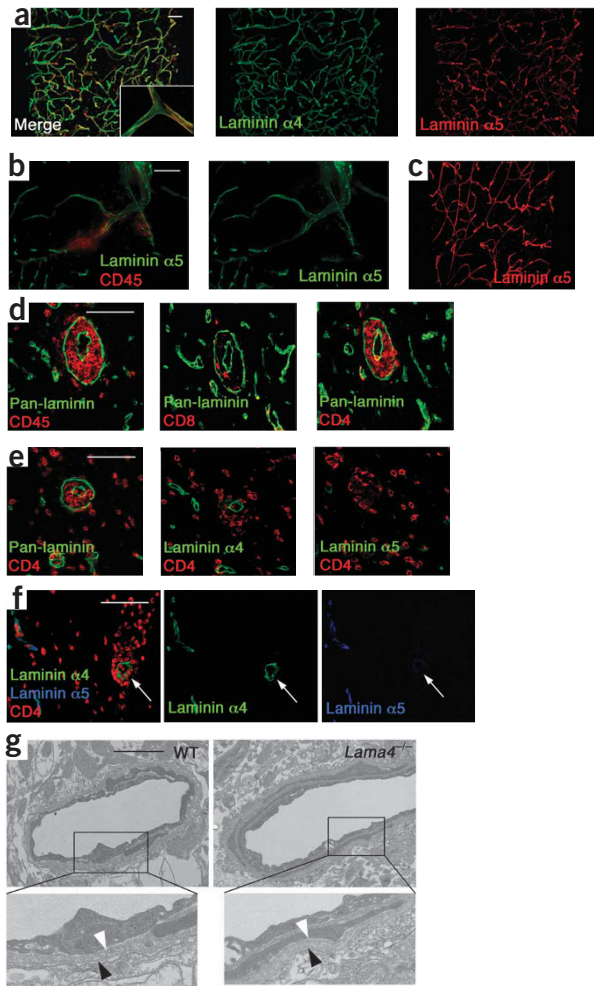


Figure 1 Immunofluorescence and electron microscopy analyses of WT and *Lama4*^{-/-} brains. (a–c) Confocal analyses of 60- to 100-µm sections of WT uninflamed brain double-stained for laminin α 4 and laminin α 5, showing also laminin α 4 and laminin α 5 alone (a), WT day 14 EAE brain double-stained for laminin α 5 and CD45 (b) and uninflamed *Lama4*^{-/-} brain stained for laminin α 5 (c). Scale bar, 40 µm. (d–f) Immunofluorescence images of consecutive 5-µm sections of inflamed WT brains double-stained for pan-laminin and CD45, CD8 or CD4 (d), double-stained for CD4 and laminin α 4 or laminin α 5 (e), or triple-stained for laminin α 4, laminin α 5 and CD4 (f). The arrow in f marks a site of extravasation. Scale bar, 40 µm. (g) Transmission electron microscopy of postcapillary venules in the CNS of a *Lama4*^{-/-} mouse and a WT littermate. Enlargements of the boxed areas illustrate endothelial basement membrane (white arrowhead) and subjacent parenchymal basement membrane (black arrowhead). Scale bar, 0.5 µm.

Using laminin α 4-deficient (*Lama4*^{-/-}) mice, which show a compensatory ubiquitous expression of laminin α 5 in all blood vessels and no differential expression in various blood vessel types nor regulatory expression of this chain in response to proinflammatory cytokines^{21,22}, we have addressed the role of endothelial basement membrane laminins in T lymphocyte extravasation in EAE. *Lama4*^{-/-} mice show markedly reduced disease susceptibility and severity compared to wild-type littermates owing to a selective reduction in T cell infiltration into the brain. We obtained similar results in mice subjected to EAE when the major laminin α 4 receptor on encephalitogenic T lymphocytes, integrin α ₆ β ₁, was genetically eliminated or functionally impaired by blocking antibodies. Collectively, the data indicate that laminin α 5 selectively inhibits α ₆ β ₁ integrin-mediated T lymphocyte migration across laminin α 4 and, to our knowledge, are the first to show an instructive role for endothelial basement membrane laminins specifically in T lymphocyte extravasation across inflamed CNS postcapillary venules. Furthermore, the data provide the rationale for targeting encephalitogenic T lymphocyte interactions with endothelial basement membrane laminins as a unique treatment to inhibit disease progression.

RESULTS

Morphology

Brain blood vessels show uniform distribution of laminin α 4 along all vessels and patchy distribution of laminin α 5 in smaller vessels with areas of little or no laminin α 5 (Fig. 1). It is these laminin α 5^{low} laminin α 4^{high} sites (Fig. 1a and **Supplementary Video 1** online) where leukocyte extravasation preferentially occurs⁷, as shown by immunofluorescence of EAE brain stained for laminin α 5 and CD45 (Fig. 1b and **Supplementary Video 2** online), CD4 or CD8 (Fig. 1d–f)⁷. In *Lama4*^{-/-} mice, laminin α 5 is expressed throughout the length of all vessels (Fig. 1c)²¹ without upregulation of the protein or of other basement membrane components (**Supplementary Fig. 1a** online). Immunofluorescence of EAE and uninflamed brains for vascular cell adhesion molecule-1 or the endothelial cell junctional proteins VE-cadherin, platelet-endothelial cell adhesion molecule-1, CD99, endothelial cell selective adhesion molecule-1 (ESAM-1) and junctional adhesion molecule-A revealed no difference between wild-type (WT) and *Lama4*^{-/-} mice (data not shown). Electron microscopy of uninflamed brains revealed distinct electron-dense endothelial and parenchymal basement membranes surrounding postcapillary venules in both WT and *Lama4*^{-/-} mice and no overt morphological alteration in vessel integrity of *Lama4*^{-/-} mice (Fig. 1g).

Active EAE

Lama4^{-/-} mice show significantly lower disease susceptibility and severity and fewer inflammatory cuffs in active EAE compared to WT littermates (Fig. 2a), suggesting reduced leukocyte infiltration.

surrounded by inflammatory cuffs, and these lymphoid chemokines have been implicated in T lymphocyte migration across the endothelial cell monolayer¹⁶. Previous studies have suggested that subsequent migration out of the perivascular cuff and into the CNS parenchyma requires the classical inflammatory chemokines, including CCL2 (refs. 12,17,18).

Although considerable information is available on the molecular mechanisms of initial penetration of the endothelial cell monolayer in EAE, little is known about how T lymphocytes subsequently traverse the endothelial basement membrane. Endothelial basement membranes are biochemically distinct from other basement membranes and are characterized by the presence of laminin-411 (composed of α 4, β 1 and γ 1 chains) and laminin-511 (α 5, β 1 and γ 1)⁵, with ubiquitous laminin- α 4 localization in all endothelial basement membranes and laminin α 5 localization predominantly in capillary and postcapillary venule basement membranes⁵. Our previous studies have shown a correlation between sites of T lymphocyte transmigration of endothelial basement membranes and the presence of laminin α 4 and low levels of laminin α 5, but little transmigration where both laminin chains occur together⁷. This observation leads to fundamental questions concerning leukocyte extravasation, including whether endothelial basement membrane components provide molecular cues that guide extravasating leukocytes. It has also been proposed that laminin-411 and laminin-511 influence T cell activation by acting as co-stimulatory molecules^{19,20}.

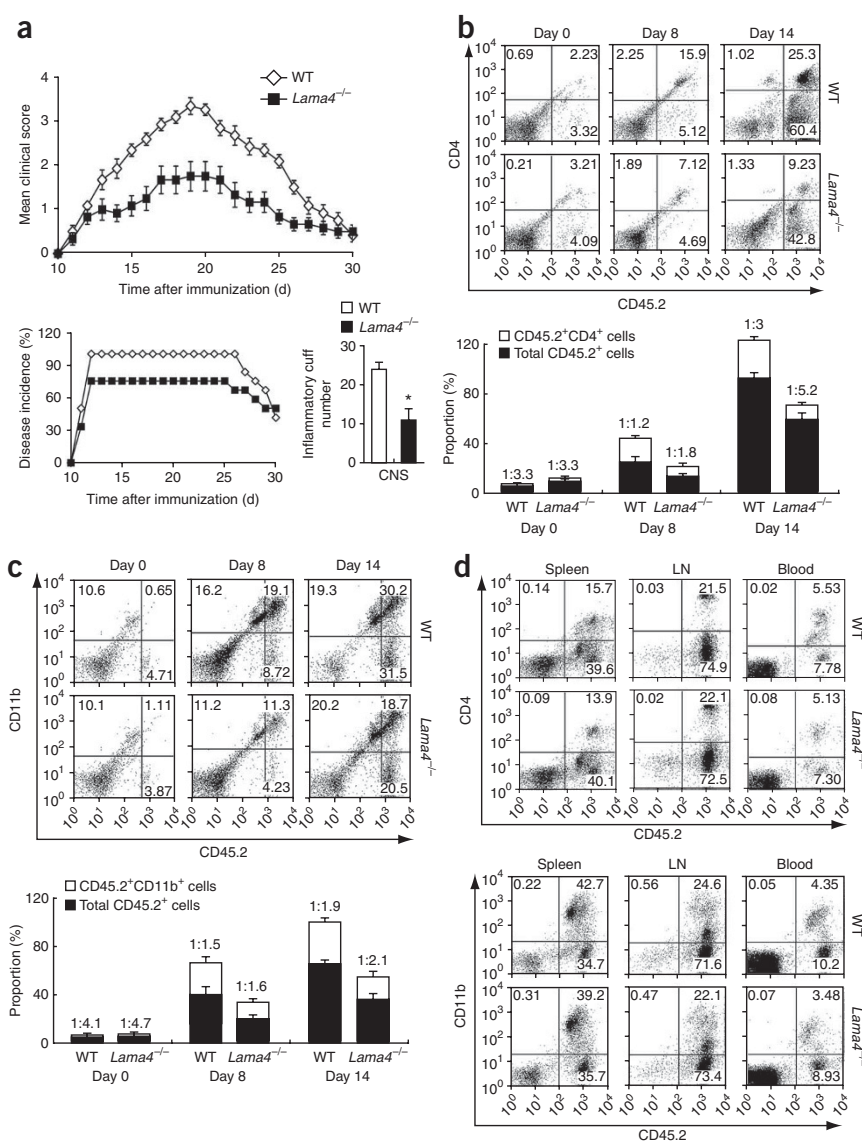


Figure 2 Active EAE induction in *Lama4*^{-/-} mice and WT littermates. **(a)** Mean clinical score \pm s.e.m. (top) and mean percentage disease incidence over time after MOG_{35–55} immunization (bottom left). Data are means of six independent experiments and at least five WT and five *Lama4*^{-/-} mice in each experiment; in both cases, $P < 0.05$. The bar graph (bottom right) shows the mean number of inflammatory cuffs per $\text{cm}^2 \pm$ s.e.m. in CNS sections of WT and *Lama4*^{-/-} mice counted in five random sections per brain and repeated with at least five individual mice ($*P < 0.05$). **(b, c)** Top, FACS analysis of total infiltrating CD45⁺CD4⁺ T lymphocytes **(b)** and total CD45^{high}CD11b⁺ macrophages **(c)** in perfused brains at days 0, 8 and 14 after active EAE induction in WT and *Lama4*^{-/-} mice. Bottom, bar graphs showing infiltrating CD4⁺ T lymphocyte or CD45^{high}CD11b⁺ macrophages expressed as percentages of total CD45⁺ infiltrating cells. The ratios of T lymphocytes to total CD45⁺ infiltrated leukocytes and macrophages to total CD45⁺ infiltrated leukocytes are given. **(d)** FACS plots showing the proportions of CD45⁺CD4⁺ (top) T lymphocytes and CD45^{high}CD11b⁺ macrophages (bottom) in spleen, lymph nodes (LN) and blood of *Lama4*^{-/-} and WT mice at day 14 after active EAE induction. FACS plots in **b–d** are one representative experiment, with each plot representing data from three mice; bar graphs in **b** and **c** are mean values \pm s.e.m. from at least six independent experiments performed with at least five WT and five *Lama4*^{-/-} mice in each experiment.

(Fig. 3a). We obtained similar results in active EAE induced in *Lama4*^{-/-} mice carrying WT bone marrow (**Supplementary Fig. 2** online), excluding immune cell defects in *Lama4*^{-/-} mice.

Use of polymorphic lineage determinants permitted quantification of passively transferred donor (CD45.1⁺) and host (CD45.2⁺) T lymphocytes. Significantly fewer donor T lymphocytes ($P < 0.05$, **Fig. 3b**) and host T lymphocytes, macrophages ($P < 0.05$, **Fig. 3c**) and DCs (data not shown) infiltrated into *Lama4*^{-/-} brains compared to WT brains. No differences were observed between *Lama4*^{-/-} and WT mice in the number of apoptotic or dead cells in the CNS (data not shown), nor were there differences in the infiltration of donor or host cells into lymph nodes or spleen (**Fig. 3b,c**). As the transferred cells were almost exclusively CD4⁺ T cells, the ratio of donor CD45.1⁺ cells to total CD45⁺ cells approximates the proportion of infiltrating donor T cells, revealing a particularly low proportion of donor CD4⁺ T cells in *Lama4*^{-/-} brains (1 in 30) compared to WT brains (1 in 16) ($P < 0.05$, **Fig. 3b**) and confirming the predominant reduction in T lymphocyte infiltration suggested in active EAE (**Fig. 2a**). Similarly, the ratio of host T lymphocytes (CD45.2⁺CD4⁺) to total CD45.2⁺ cells was 1 in 3 in WT brains versus 1 in 5 in *Lama4*^{-/-} brains ($P < 0.05$, **Fig. 3c**). Although host macrophage numbers in *Lama4*^{-/-} brains were lower than in WT littermates, when these numbers were expressed as the proportion of total infiltrating CD45.2⁺ cells, there was no significant difference between *Lama4*^{-/-} and WT mice (**Fig. 3c**). No CD45.2⁺CD8⁺ T lymphocytes were detectable in WT or *Lama4*^{-/-} brains (data not shown).

FACS revealed lower counts of CD45⁺ cells, CD8⁺ and CD4⁺ T cells, CD11b⁺ macrophages and CD11c⁺ dendritic cells (DCs; data not shown) in *Lama4*^{-/-} compared to WT brains on days 8 and 14 after EAE induction (**Fig. 2b,c**), but not in draining lymph nodes, spleens or the circulation (**Fig. 2d**). When expressed as a ratio of total infiltrating CD45⁺ cells, it was apparent that the lower infiltration into *Lama4*^{-/-} brains was most pronounced for the disease-inducing CD4⁺ T lymphocytes ($P < 0.05$, **Fig. 2b**) and not for CD8⁺ T cells, which represented a low proportion of total infiltrated leukocytes (2–3%).

Passive EAE

As laminin $\alpha 4$ and laminin $\alpha 5$ were reported to be expressed by human T lymphocytes and to act as cofactors for T cell activation^{19,20}, we investigated laminin expression in mouse and in human T lymphocytes and T lymphocyte ontogeny and activation in *Lama4*^{-/-} mice using passive transfer experiments. We did not detect laminin $\alpha 4$ or laminin $\alpha 5$ in naive or activated mouse or human CD4⁺ T lymphocytes via previously described protocols^{19,20} (**Supplementary Fig. 1b–d**). Transfer of WT encephalitogenic T cells to *Lama4*^{-/-} recipients resulted in significantly reduced disease incidence (data not shown, $P < 0.05$) and severity compared to WT recipients

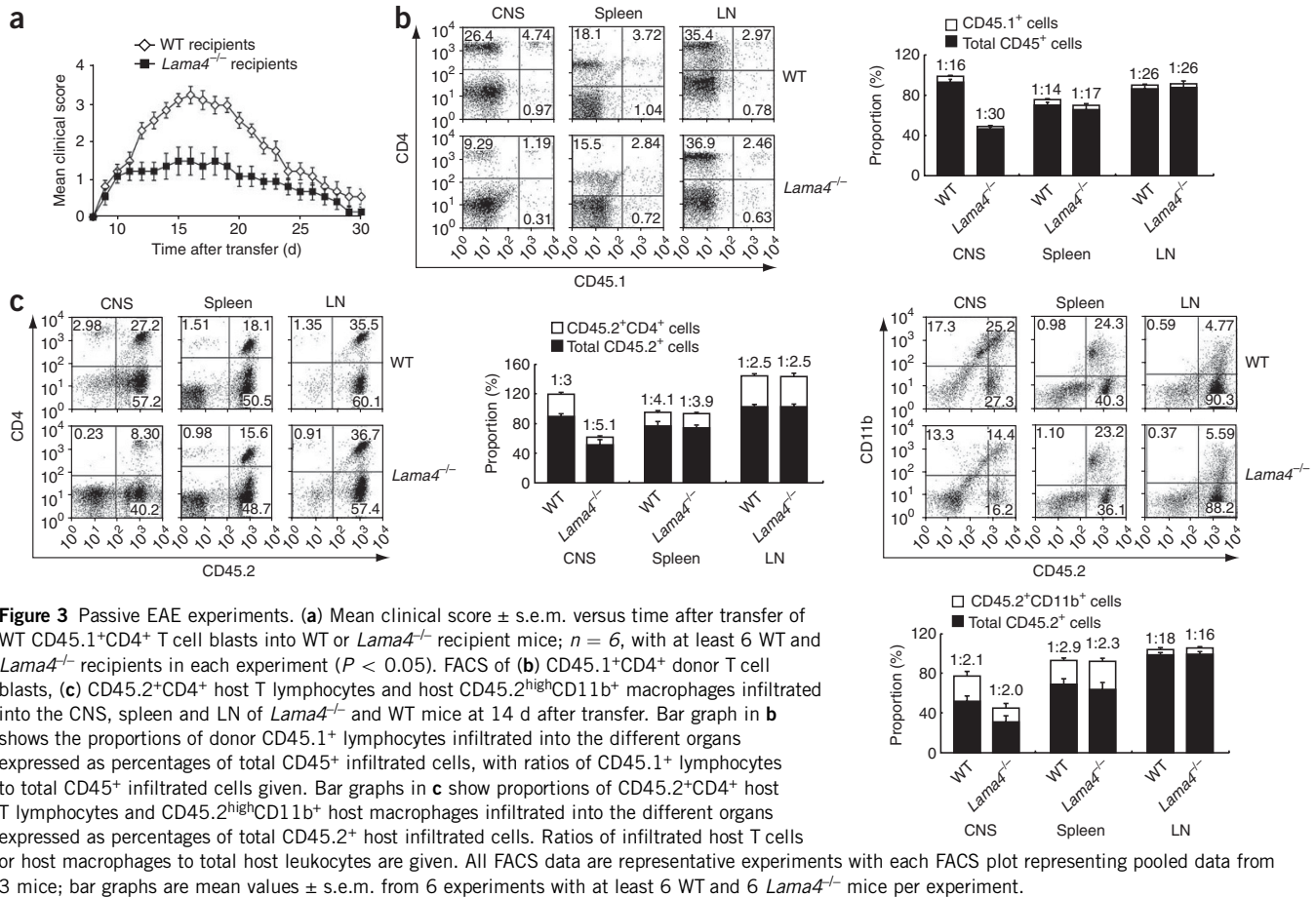


Figure 3 Passive EAE experiments. **(a)** Mean clinical score \pm s.e.m. versus time after transfer of WT CD45.1⁺CD4⁺ T cell blasts into WT or *Lama4*^{-/-} recipient mice; $n = 6$, with at least 6 WT and *Lama4*^{-/-} recipients in each experiment ($P < 0.05$). FACS of **(b)** CD45.1⁺CD4⁺ donor T cell blasts, **(c)** CD45.2⁺CD4⁺ host T lymphocytes and host CD45.2^{high}CD11b⁺ macrophages infiltrated into the CNS, spleen and LN of *Lama4*^{-/-} and WT mice at 14 d after transfer. Bar graph in **b** shows the proportions of donor CD45.1⁺ lymphocytes infiltrated into the different organs expressed as percentages of total CD45⁺ infiltrated cells, with ratios of CD45.1⁺ lymphocytes to total CD45⁺ infiltrated cells given. Bar graphs in **c** show proportions of CD45.2⁺CD4⁺ host T lymphocytes and CD45.2^{high}CD11b⁺ host macrophages infiltrated into the different organs expressed as percentages of total CD45.2⁺ host infiltrated cells. Ratios of infiltrated host T cells or host macrophages to total host leukocytes are given. All FACS data are representative experiments with each FACS plot representing pooled data from 3 mice; bar graphs are mean values \pm s.e.m. from 6 experiments with at least 6 WT and 6 *Lama4*^{-/-} mice per experiment.

T lymphocyte proliferation

To measure *in vivo* proliferation of T cells specific for the 35–55 peptide of myelin oligodendrocyte glycoprotein (MOG_{35–55}), we transferred CD45.1⁺CD4⁺ T cell blasts into CD45.2⁺ WT and *Lama4*^{-/-} mice and measured BrdU incorporation into the CD45.1⁺CD4⁺ population on day 14 after transfer (peak disease severity). No difference in the proportion of proliferating infiltrated CD45.1⁺CD4⁺ T cells was measured in WT and *Lama4*^{-/-} brains, lymph nodes or spleen (**Fig. 4a**). As expected, the degree of infiltration of MOG_{35–55}-specific CD45.1⁺CD4⁺ T cells was low only in *Lama4*^{-/-} brains, but those cells that did infiltrate had the same proliferative capacity as those that had infiltrated WT brains (**Fig. 4a**). Similar results were obtained with carboxyfluorescein succinimidyl ester-labeled ovalbumin-specific CD4⁺ T cells (OT-II cells) transferred to *Lama4*^{-/-} or WT mice who were subsequently immunized with ovalbumin (**Supplementary Fig. 3** online). *In vitro* proliferation assays confirmed the absence of defects in T cell proliferation or antigen presentation in *Lama4*^{-/-} mice (**Fig. 4b** and **Supplementary Fig. 4** online).

In vivo and *in vitro* transmigration assays

Low T lymphocyte numbers in *Lama4*^{-/-} brains in EAE plus the absence of general defects in T lymphocytes (**Supplementary Fig. 5** online) or in induction of an immune response in *Lama4*^{-/-} mice suggests a defect at the level of T lymphocyte migration across CNS postcapillary venules. We investigated this hypothesis by passive transfer of CD45.1⁺ T cells to CD45.2⁺ WT or *Lama4*^{-/-} recipients and measurement of infiltrated CD45.1⁺CD4⁺ cells at day 3 after

transfer, before commencement of T cell proliferation²³. FACS revealed identical amounts of donor T cells in the periphery of *Lama4*^{-/-} and WT mice but significantly lower numbers of donor CD45.1⁺CD4⁺ cells in *Lama4*^{-/-} compared to WT brains (**Fig. 5a,b**), indicating slower penetration of *Lama4*^{-/-} CNS postcapillary venules.

To determine why T lymphocyte migration across *Lama4*^{-/-} CNS vessels is impaired, we used *in vitro* transmigration assays. The complex three-dimensional laminin network of basement membranes *in vivo* cannot be recapitulated in transwell assays; however, the effects of laminin $\alpha 4$ - versus laminin $\alpha 5$ -mediated signals on T cell migration can be assessed, as can integrin receptor involvement. To mimic the *in vivo* situation, we used primary migration-competent splenic T lymphocytes²⁴ from WT mice actively induced for EAE, and we induced transmigration across vascular (laminin-411 and laminin-511) and nonvascular (laminin-111) laminins with CCL2 (ref. 12), CCL19 (ref. 12) or CCL21 (ref. 16).

T lymphocytes migrated most extensively across laminin-411-, laminin-111- or BSA-coated filters, with minimal migration across laminin-511 (**Fig. 5c**). As the same pattern of results was observed with CCL2, CCL19 and CCL21, data is shown only for CCL19. Function-blocking antibodies against integrins $\alpha 6$ and $\beta 1$ inhibited transmigration across laminin-411 (**Fig. 5c**), whereas the minimal migration across laminin-511 was not affected by antibodies specific for integrin $\alpha 6$, integrin $\beta 1$ or integrin $\beta 3$ (**Fig. 5c**). Transmigration across laminin-411-coated filters was reduced by increasing proportions of laminin-511, but not laminin-111, in a dose-dependent manner (**Fig. 5d**), suggesting that laminin $\alpha 5$ actively inhibits $\alpha 6\beta 1$ integrin-mediated transmigration across laminin $\alpha 4$.

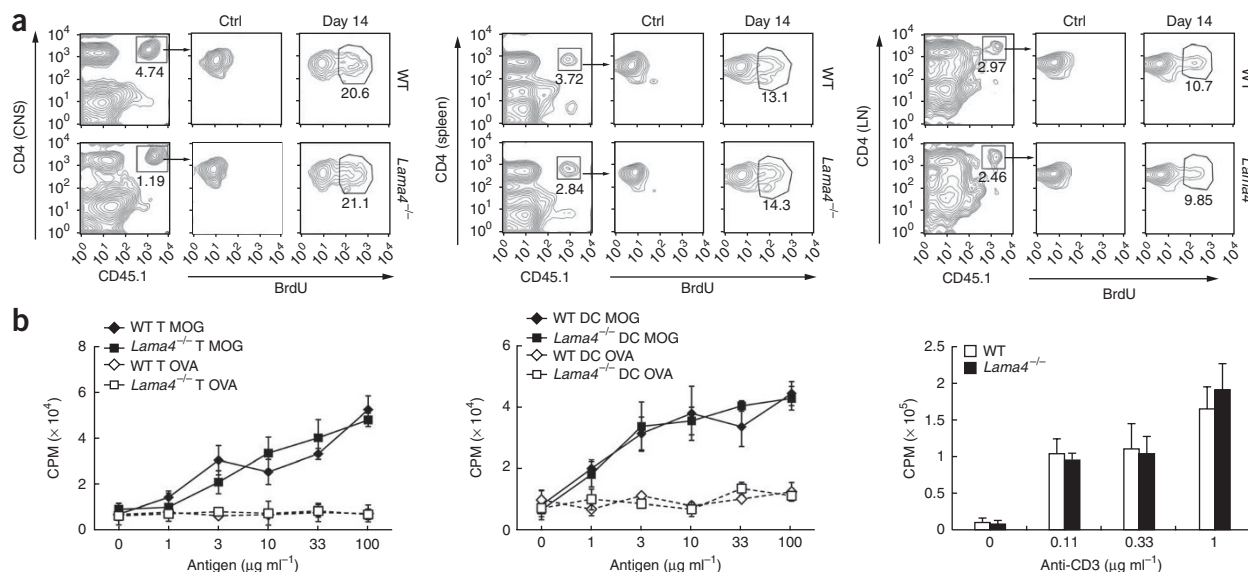


Figure 4 T lymphocyte proliferation studies. **(a)** FACS quantification of BrdU incorporation into passively transferred MOG_{35–55}-specific CD4⁺CD45.1⁺ T lymphocytes that had infiltrated into the CNS (left), spleen (middle) and LN (right) of *Lama4*^{-/-} mice and WT littermates at day 14 after transfer. Data are from one representative experiment in which three WT and three *Lama4*^{-/-} mice were used; experiments were repeated three times. **(b)** *In vitro* proliferation: all experiments were performed with WT or *Lama4*^{-/-} T lymphocytes isolated from LN at day 10 after immunization with MOG_{35–55}. Left, ³H-thymidine incorporation (CPM) into WT and *Lama4*^{-/-} T lymphocytes using irradiated WT splenic DCs as APCs. Proliferation in response to MOG_{35–55} and a nonspecific antigen, ovalbumin (OVA), was measured. Middle, ³H-thymidine incorporation into WT T lymphocytes using irradiated splenic DCs isolated from either WT or *Lama4*^{-/-} mice as APCs. Right, ³H-thymidine incorporation of WT and *Lama4*^{-/-} T lymphocytes in response to antibody to CD3 (Anti-CD3). Data are shown as means ± s.e.m.

Physiologically relevant transmigration assays for macrophages would require isolation of blood monocytes from EAE mice, which are extremely low in number. Hence, for our experiments we used activated macrophages from EAE spleens and lymph nodes, revealing an integrin-independent mode of transmigration across all substrates (Fig. 5c), indicating fundamental differences between macrophage and T lymphocyte migratory mechanisms.

Integrin α_6 bone marrow chimeric mice

As $\alpha_6\beta_1$ integrin on encephalitogenic T cells is the only receptor required for migration across laminin-411 and is not required for T cell function or leukocyte recruitment in the periphery²⁵, we investigated whether its elimination on T cells results in the same reduced EAE severity and selective reduction in T cell infiltration into the CNS as observed in *Lama4*^{-/-} mice. Because integrin α_6 -deficient (*Itga6*^{-/-}) mice die perinatally²⁶, we generated *Itga6*^{-/-} bone marrow-chimeric mice. *In vitro* activation experiments performed on the *Itga6*^{-/-} bone marrow-chimeric mice confirmed the absence of defects in T cell activation or antigen-presenting cell (APC) function (data not shown). However, the *Itga6*^{-/-} bone marrow chimeras showed lower EAE severity compared to WT mice carrying *Itga6*^{+/+} bone marrow (Fig. 6a), and FACS revealed a selective reduction in *Itga6*^{-/-} CD4⁺ T cells in the CNS ($P < 0.05$, Fig. 6b). No differences between WT mice carrying *Itga6*^{-/-} bone marrow and WT mice carrying *Itga6*^{+/+} bone marrow were observed in T cell, macrophage or DC recruitment to the lymph nodes, spleen or the circulation (Fig. 6b). When we functionally blocked integrin α_6 by systemic application of the neutralizing antibody GoH3 in mice with active induction of EAE, disease symptoms were suppressed, appearing only when circulating levels of GoH3 dropped below detection (Fig. 6c). The more efficient blocking of EAE symptoms in the antibody treatment experiments compared to the bone marrow chimera studies probably

reflects some functional compensation that can develop in the bone marrow-chimeric mice. Taken together, these data indicate that direct interaction between $\alpha_6\beta_1$ integrin on the surface of infiltrating CD4⁺ T lymphocytes and laminin-411 in the endothelial basement membrane facilitates extravasation and that the reduced CD4⁺ T cell infiltration into *Lama4*^{-/-} brains is not due to a secondary effect.

DISCUSSION

In addition to and penetration of the endothelial cell monolayer, encephalitogenic T lymphocyte interaction with endothelial basement membrane laminins represents a key rate-limiting step in the initial stages of EAE development. Our previous work suggested that the laminin composition of endothelial basement membrane determines sites of leukocyte extravasation in EAE, with transmigration occurring preferentially where laminin α_4 was present and laminin α_5 expression was low⁷. Data presented here indicate that this is due to an inhibitory affect of laminin α_5 on integrin $\alpha_6\beta_1$ -mediated T lymphocyte migration across laminin α_4 -containing basement membranes. Elimination of laminin α_4 or its major receptor, integrin $\alpha_6\beta_1$, resulted in the same reduced T cell infiltration into the CNS and thereby reduced EAE severity and susceptibility, suggesting that direct interaction between infiltrating CD4⁺ T lymphocytes and laminin-411 in the endothelial basement membrane facilitates extravasation. However, as laminin α_4 is ubiquitously expressed along the vascular tree and $\alpha_6\beta_1$ is strongly expressed on all T lymphocytes, laminin α_4 and integrin $\alpha_6\beta_1$ alone are insufficient to explain the focal extravasation pattern observed in EAE. Rather, our data suggest that this focal extravasation is due to the patchy distribution of laminin α_5 in the endothelial basement membrane of postcapillary venules and its inhibitory effect on T lymphocyte transmigration. Notably, the data indicate that different leukocyte

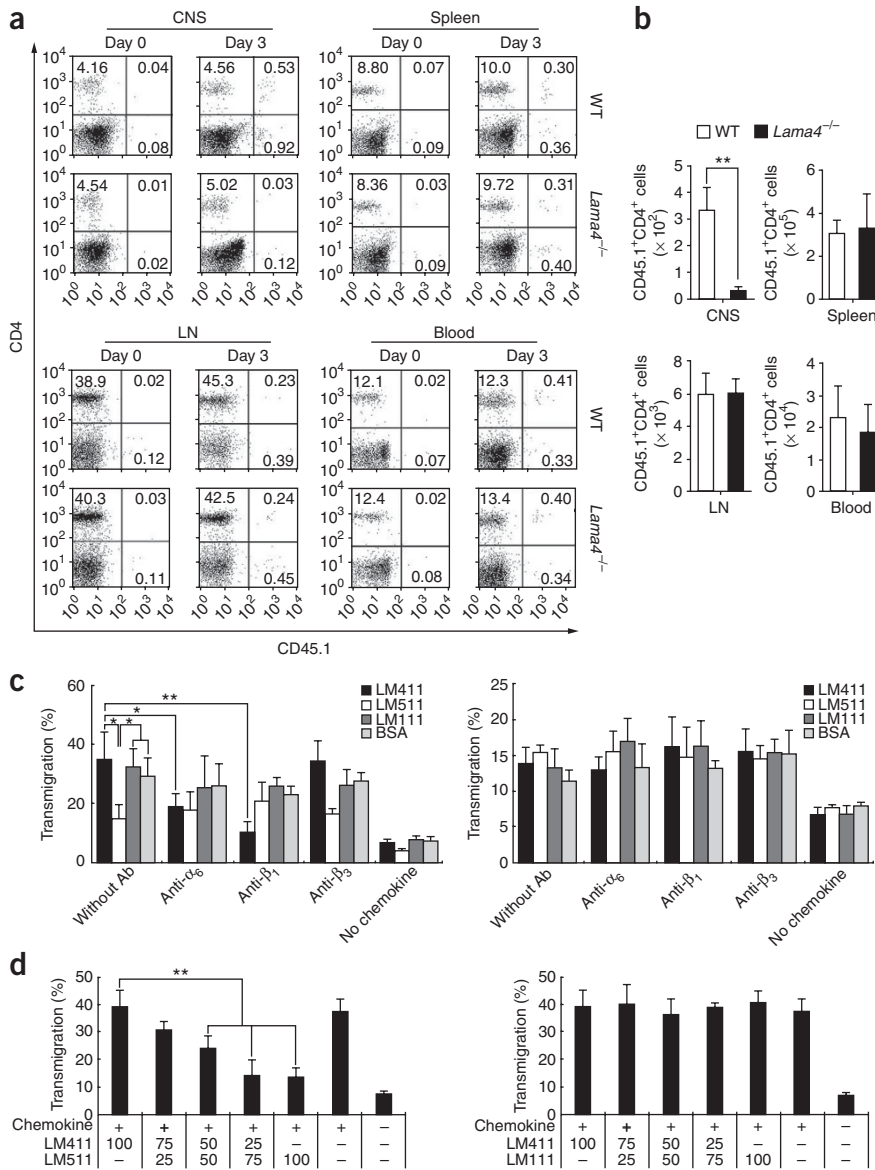


Figure 5 Encephalitogenic T lymphocyte transmigration studies. **(a)** *In vivo* migration studies showing CD45.1⁺CD4⁺ donor T lymphocytes in perfused brains (CNS), LN, spleen and blood at days 0 and 3 after transfer, as measured by FACS. **(b)** Quantification of T lymphocyte *in vivo* transmigration studies. **(c)** Quantification of CCL19-induced transmigration of primary encephalitogenic T lymphocytes (left) or CCL3-induced transmigration of primary macrophages (right) from day 14 EAE spleens across transwell filters coated with laminin-411, laminin-511, laminin-111 or BSA in the presence and absence of function-blocking antibodies to integrins α_6 , β_1 and β_3 . **(d)** CCL19-induced transmigration of primary T lymphocytes across filters coated with the indicated percentages of laminin-411 and laminin-511 (left) or laminin-411 and laminin-111 (right). Data in **c** and **d** are for WT T cells; similar results were obtained for *Lama4*^{-/-} T cells. Data in **a** is a representative FACS; data in **b–d** are mean values \pm s.e.m. from six experiments with at least triplicate data points per experiment. **P* < 0.05 and ***P* < 0.01.

The only overt alteration in the *Lama4*^{-/-} mouse is the compensatory switch to widespread laminin α_5 distribution in all endothelial basement membranes without overexpression^{21,29,30}. Clearly, changes in laminin isoform composition of endothelial basement membranes alter the internetwork (within the laminin network) and intranetwork (between laminins and other basement membrane components) interactions and thereby the tightness of the network^{31,32}. Such ultrastructural alterations are likely to account for the lower levels of migration of both T cells and macrophages across laminin α_5 -containing vascular basement membranes into the CNS but not the more pronounced reduction in activated CD4⁺ T cell infiltration. This indicates not only that basement

membrane architecture is a limiting factor in the transmigration process but also that activated CD4⁺ T lymphocytes use different mechanisms than macrophages, DCs and CD8⁺ T cells³³ to migrate across basement membranes, and these mechanisms are determined by the basement membrane laminin composition. This supports previous studies demonstrating that CD4⁺ and CD8⁺ T cells use different mechanisms to infiltrate into the CNS in EAE³³.

Passive transfer of WT encephalitogenic T cells to WT or *Lama4*^{-/-} recipients and analysis of their distribution in the periphery and CNS at day 3 after transfer, before any *in vivo* proliferation, revealed lower rates of T cell migration specifically into the CNS of *Lama4*^{-/-} mice. As the only alteration in these *Lama4*^{-/-} mice is the expression of laminin α_5 in the endothelial basement membrane of the postcapillary venule, this is strong evidence for an inhibitory role for laminin α_5 in T cell transmigration. This possibility was substantiated by *in vitro* migration assays with primary encephalitogenic T cells, which showed substantial chemokine-induced migration across laminin α_4 only and specific inhibition of this migration by increasing the ratio of laminin α_5 to laminin α_4 .

types use distinct mechanisms to penetrate the endothelial basement membrane, providing a potential means of targeting specific infiltrating leukocyte populations.

The lower disease severity in *Lama4*^{-/-} mice was due to lower levels of infiltration of most leukocytes known to have a role in EAE, including DCs, macrophages and T cells, but with a predominant effect on the disease-inducing CD4⁺ T lymphocytes. Electron microscopic and immunofluorescence analyses of *Lama4*^{-/-} brains revealed no defects in the integrity of the endothelial cell monolayer or its underlying basement membrane, nor did we detect aberrant expression of endothelial cell adhesion or junctional molecules that have been implicated in the transmigration process^{4,27,28}. Further, the normal course of active EAE in WT mice carrying *Lama4*^{-/-} bone marrow indicates the absence of defects in T cell or APC ontogeny or function in *Lama4*^{-/-} mice, which was substantiated by the normal *in vitro* and *in vivo* activation of *Lama4*^{-/-} T cells. Rather, the lower disease incidence and severity observed in active EAE in *Lama4*^{-/-} mice carrying WT bone marrow and in *Lama4*^{-/-} mice passively transferred with WT encephalitogenic T lymphocytes strongly suggest impaired T cell extravasation across *Lama4*^{-/-} CNS postcapillary venules.

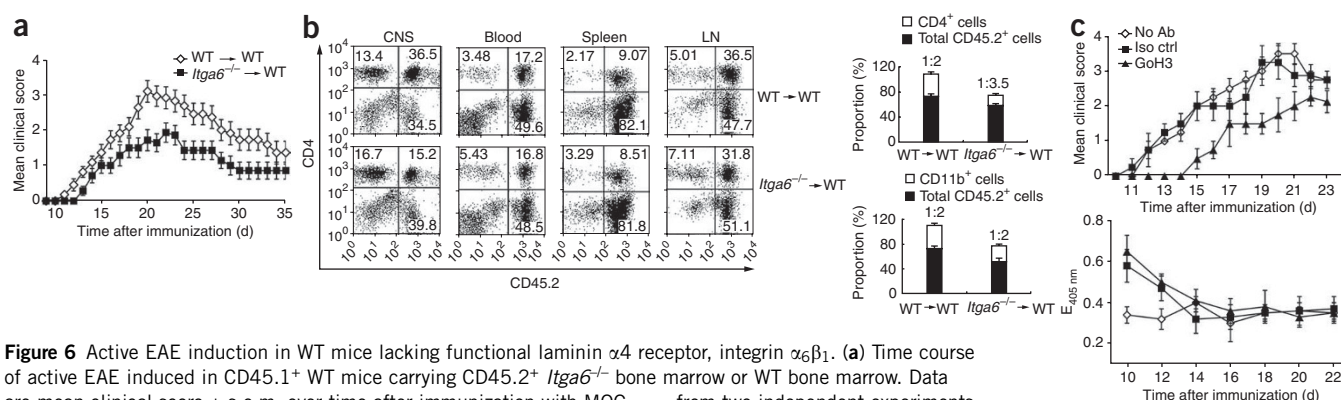


Figure 6 Active EAE induction in WT mice lacking functional laminin $\alpha 4$ receptor, integrin $\alpha 6\beta 1$. **(a)** Time course of active EAE induced in CD45.1⁺ WT mice carrying CD45.2⁺ *Itga6*^{-/-} bone marrow or WT bone marrow. Data are mean clinical score \pm s.e.m. over time after immunization with MOG₃₅₋₅₅ from two independent experiments with 12 *Itga6*^{-/-} and 12 WT bone marrow chimeric mice in each experiment ($P < 0.003$). **(b)** Left, FACS analysis of CD45.2⁺CD4⁺ T lymphocytes infiltrated into the CNS, LN, spleen and blood at day 14 after active EAE induction (peak severity). Right, bar graphs showing quantification of infiltrating CD45.2⁺CD4⁺ T lymphocytes (top) or CD45.2⁺CD11b⁺ macrophages (bottom) expressed as percentages of total CD45.2⁺ infiltrating cells. **(c)** Top, time course of active EAE induced in WT mice injected i.v. with antibody to integrin $\alpha 6\beta 1$ (GoH3), an isotype control antibody (Iso ctrl) or PBS alone (No Ab) at days 1, 3, 5 and 7 after immunization with MOG₃₅₋₅₅. Bottom, corresponding ELISA for serum levels of GoH3 or control IgG, showing emission at 405 nm (E_{405 nm}). Data are mean clinical score \pm s.e.m. over time after immunization with MOG₃₅₋₅₅ from two independent experiments with five control and four antibody-treated mice in each experiment.

Chemokine-induced migration of primary encephalitogenic T cells across laminin-411 was reduced to baseline levels by blocking integrin $\alpha 6\beta 1$, consistent with previous reports of $\alpha 6\beta 1$ integrin as a major laminin-411 receptor^{34,35}. The fact that *Itga6*^{-/-} bone marrow chimeric mice show the same reduced EAE susceptibility and disease severity as *Lama4*^{-/-} mice and the same selective reduction in T lymphocyte infiltration into the CNS strongly suggests that direct interaction between the infiltrating encephalitogenic T cells and laminin-411 facilitates CD4⁺ T cell penetration of the endothelial basement membrane. Given that laminin $\alpha 4$ is expressed throughout the vascular tree and $\alpha 6\beta 1$ integrin is highly expressed on encephalitogenic T cells, extravasation could occur at any site. The fact that it does not and occurs focally is explained by the inhibitory role of laminin $\alpha 5$ and its patchy distribution in post-capillary venules⁷.

Once within the CNS, MOG₃₅₋₅₅-specific T cells have the same proliferative capacity regardless of whether they are in a *Lama4*^{-/-} or WT environment, indicating normal re-stimulation of T lymphocytes. Similarly, the survival of MOG₃₅₋₅₅-specific T cells in a *Lama4*^{-/-} or WT CNS does not differ. These results are not surprising, as there is no laminin $\alpha 4$ expressed within the CNS parenchyma. Of note, *in vitro* proliferation studies have shown that both microglia and astrocytes are not as effective as DCs and APCs³⁶, supporting previous studies suggesting that infiltrated DCs are the major APCs within the CNS.

The fact that endothelial basement membrane laminin composition specifically influences the transmigration of T lymphocytes raises the possibility of targeting T lymphocyte interactions with endothelial laminins as a new therapeutic strategy to inhibit neuroinflammatory processes without compromising unspecific immune responses. We showed that this is a feasible therapeutic approach by suppressing EAE symptoms through systemic treatment with the integrin $\alpha 6$ -specific antibody, GoH3, as disease symptoms appeared concurrently with reduced circulating concentrations of the antibody. Hence, although targeting molecules such as integrin $\alpha 4$ as multiple sclerosis therapy may efficiently reduce leukocyte trafficking to the CNS³⁷, targeting of integrin $\alpha 6\beta 1$ -laminin $\alpha 4$ -mediated interactions may represent a more selective means of decreasing extravasation of activated CD4⁺ T lymphocytes across CNS vessels.

METHODS

Mice. We used *Lama4*^{-/-} mice²¹ backcrossed at least 16 times onto a C57BL/6 background (Charles River Laboratories). Experiments were conducted according to German animal welfare guidelines and approved by Landesamt fuer Natur, Umwelt und Verbraucherschutz Nordrhein Westfalen (permit 50.0835.1.0).

Antibodies. We used the following antibodies: rabbit antibodies to mouse laminin $\alpha 4$ (377), laminin $\alpha 5$ (405) and panlaminin (455)⁷, ESAM-1 (provided by D.V.), CD99 (ref. 38), junctional adhesion molecule-A (provided by D.V.)³⁹ and platelet-endothelial cell adhesion molecule-1 (MEC13.3, Pharmingen) and rat antibodies to mouse laminin $\alpha 5$ (4G6)⁴⁰, vascular cell adhesion molecule-1 (M/K-2, Southern Biotech), CD45 (30G.12, Pharmingen), CD45.2 (104, eBiosciences), CD45.1 (A20, Pharmingen), CD11b (M1/70, Pharmingen), CD4 (H129.19, Pharmingen), CD8 (53-6.7, eBiosciences), integrin $\beta 1$ (Ha2/5, Pharmingen), integrin $\beta 3$ (2C9.G2, Pharmingen) and integrin $\alpha 6$ (GoH3, Pharmingen). Antibodies to laminin were made in house.

Morphological analyses. We performed electron microscopy with standard protocols. We performed immunofluorescence as previously described⁴⁰. We examined sections with a Zeiss AxioImager microscope equipped with epifluorescent optics and documented them with a Hamamatsu ORCA ER camera or with a Zeiss confocal laser scanning system LSM 510 meta. We analyzed images with Volocity 4.4 software (Improvision).

Active experimental autoimmune encephalitis. We induced EAE in female C57BL/6 mice using MOG₃₅₋₅₅ (Schaefer-N) as previously described⁷.

In some experiments, we intravenously (i.v.) injected function-blocking antibody to integrin $\alpha 6$ (GoH3), isotype control antibody (IgG2a) (100 μ g per mouse) or PBS alone into WT mice at days 1, 3, 5 and 7 after MOG₃₅₋₅₅ immunization. We analyzed sera daily for GoH3 or control IgG2a titers by ELISA using recombinant integrin $\alpha 6\beta 1$ or rat IgG (1 μ g ml⁻¹) as substrates.

Passive experimental autoimmune encephalitis. We stimulated 1×10^7 cells per ml from lymph nodes of MOG₃₅₋₅₅-immunized mice with 20 μ g ml⁻¹ MOG₃₅₋₅₅ for 2 d and then 20 ng ml⁻¹ interleukin-2 for 3 d. On day 5, we added 10 ng ml⁻¹ interleukin-23 and cultured the cells for another 5 d before we transferred T cell blasts i.v. to host mice. We injected 20 ng pertussis toxin intraperitoneally on the day of transfer and on day 2. We used polymorphic lineage determinants (CD45.1 or CD45.2) for tracking donor versus host immune cells.

Bone marrow-chimeric mice. We transferred bone marrow cells i.v. (5×10^6 per mouse) to lethally irradiated (11 Gy) congenic recipient mice. We used

polymorphic lineage determinants (CD45.1 or CD45.2) for tracking donor-derived versus host-derived immune cells. We generated *Itga6*^{-/-} (ref. 26) bone marrow–chimeric mice with *Itga6*^{-/-} fetal liver cells. We used mice with >95% donor cell engraftment in EAE experiments.

T lymphocyte proliferation assays. For *in vitro* T lymphocyte proliferation assays, we cultured CD4⁺ T lymphocytes from lymph nodes of MOG_{35–55}–immunized mice at 37 °C for 3 d with irradiated splenic DCs (from nonimmunized mice) plus MOG_{35–55} or the ovalbumin fragment 323–339 (OVA_{323–339}) (Schafer-N), or with antibody to CD3 (Pharminogen). We determined T lymphocyte proliferation by ³H-thymidine (Amersham) incorporation over 12 h. We cocultured WT or *Lama4*^{-/-} T lymphocytes with WT or *Lama4*^{-/-} splenic DCs in separate experiments. We performed similar experiments with *Itga6*^{-/-} T cells and WT APCs. For *in vivo* T lymphocyte proliferation assays, we transferred encephalitogenic T cell blasts (CD45.1⁺) i.v. to WT or *Lama4*^{-/-} mice (CD45.2⁺) and injected BrdU intraperitoneally on days 11 and 13 after transfer. We removed the lymph nodes, spleen and CNS 12 h after the last injection, isolated CD45.1⁺CD4⁺ T lymphocytes and analyzed them for BrdU incorporation by FACS.

Fluorescence-activated cell sorting. We perfused mice with PBS before we collected the spleens, lymph nodes and brains. We treated spleens and lymph nodes with 2 mg ml⁻¹ collagenase D and 1 mg ml⁻¹ DNase I (Roche Diagnostics), and we isolated total cells by cell sieving (70 μm). We separated brain homogenates into neuronal and leukocyte populations by discontinuous density gradient centrifugation using isotonic Percoll (Amersham)⁴¹. We performed FACS using a FACSCalibur (Becton Dickinson) with the antibodies listed above.

Transmigration assays. We coated transwell filters (5 μm, Costar) overnight at 4 °C with 10 μg ml⁻¹ of purified laminin-411, laminin-511, laminin-111 (ref. 42) or with various ratios of laminin-411 and laminin 511 or laminin-411 and laminin-111 (final concentration was maintained constant at 10 μg ml⁻¹). We blocked the filters with 1% BSA in PBS, and we placed 6 × 10⁵ splenic CD4⁺ T lymphocytes from MOG_{35–55}–immunized mice in serum-free RPMI in the upper chamber. We induced transmigration with 500 ng ml⁻¹ CCL19, CCL21 or CCL2 (PromoKine) in serum-free RPMI in the lower chamber¹⁶. We conducted the experiments at 37 °C for 4 h, counted transmigrated cells and quantified them as a percentage of total cells added. In some cases, we preincubated cells with 25 μg ml⁻¹ antibodies to integrin β₁, integrin β₃ or integrin α₆ before adding them to the upper chamber. We performed similar experiments with macrophages isolated from spleens and lymph nodes of MOG_{35–55}–immunized mice, except that we used 8-μm Transwell filters and 250 ng ml⁻¹ CCL3 or CCL2 as chemoattractants.

Statistical analyses. We used a paired sign *t* test or Student's *t* test. We considered *P* values of 0.05 or less statistically significant.

Note: Supplementary information is available on the Nature Medicine website.

ACKNOWLEDGMENTS

This work was supported by the German (SFB293 A14, B8, A1; SFB492 Z3) and Swedish Research Councils (K2005-06X-14184-04A, 621-2001-2142), Alfred Österlunds Foundation, Knut and Alice Wallenbergs Foundation (KAW 2002.0056), the Crafoord Foundation, the Greta and Johan Kocks Foundation and the Interdisciplinary Clinical Research Center (IZKF; Lo2/017/07) in Münster, Germany. We thank M. Sixt for initial studies on *Lama4*^{-/-} mice, J. Eble (Frankfurt University) for recombinant integrin α₆β₁, A. Sonnenberg (Division of Cell Biology, The Netherlands Cancer Institute) for GoH3, A. De Arcangelis for tissue collection, G. Roos for technical assistance and F. Kiefer and R. Böhmer for assistance with confocal microscopy.

AUTHOR CONTRIBUTIONS

All experimental work was carried out by C.W. P.A. and F.I. contributed to the *in vivo* and *in vitro* T lymphocyte proliferation studies; P.N. was instrumental in generation of bone marrow–chimeric mice; H.R. carried out all electron microscopy studies; the *Lama4*^{-/-} mouse was generated in K.T.'s laboratory; R.H. was instrumental in project development and experimental design; D.V. provided expertise and tools for assessment of endothelial cell-to-cell contacts in *Lama4*^{-/-} mice; K.L., S.B. and J.S. provided expertise and tools for FACS analyses; E.K.

carried out immunofluorescence analyses; E.G.-L. provided the *Itga6*^{-/-} embryonic liver cells for generation of bone marrow–chimeric mice; project development and all experimental work was carried out under the supervision and in the laboratory of L.M.S.

Published online at <http://www.nature.com/naturemedicine/>

Reprints and permissions information is available online at <http://npng.nature.com/reprintsandpermissions/>

- Ohashi, K.L., Tung, D.K., Wilson, J., Zweifach, B.W. & Schmid-Schonbein, G.W. Transvascular and interstitial migration of neutrophils in rat mesentery. *Microcirculation* **3**, 199–210 (1996).
- Hoshi, O. & Ushiki, T. Neutrophil extravasation in rat mesenteric venules induced by the chemotactic peptide *N*-formyl-methionyl-leucylphenylalanine (fMLP), with special attention to a barrier function of the vascular basal lamina for neutrophil migration. *Arch. Histol. Cytol.* **67**, 107–114 (2004).
- Yadav, R., Larbi, K.Y., Young, R.E. & Nourshargh, S. Migration of leukocytes through the vessel wall and beyond. *Thromb. Haemost.* **90**, 598–606 (2003).
- Bixel, M.G. *et al.* A CD99-related antigen on endothelial cells mediates neutrophil but not lymphocyte extravasation *in vivo*. *Blood* **109**, 5327–5336 (2007).
- Hallmann, R. *et al.* Expression and function of laminins in the embryonic and mature vasculature. *Physiol. Rev.* **85**, 979–1000 (2005).
- Engelhardt, B. Lymphocyte trafficking through the central nervous system. in *Adhesion Molecules and Chemokines in Lymphocyte Trafficking* (ed. Hamann, A.) 173–200 (Harwood Academic Publishers, Amsterdam, 1997).
- Sixt, M. *et al.* Endothelial cell laminin isoforms, laminin 8 and 10, play decisive roles in T-cell recruitment across the blood-brain-barrier in an experimental autoimmune encephalitis model (EAE). *J. Cell Biol.* **153**, 933–946 (2001).
- Agrawal, S. *et al.* Dystroglycan is selectively cleaved at the parenchymal basement membrane at sites of leukocyte extravasation in experimental autoimmune encephalomyelitis. *J. Exp. Med.* **203**, 1007–1019 (2006).
- Kawakami, N. *et al.* Live imaging of effector cell trafficking and autoantigen recognition within the unfolding autoimmune encephalomyelitis lesion. *J. Exp. Med.* **201**, 1805–1814 (2005).
- Wang, S. *et al.* Venular basement membranes contain specific matrix protein low expression regions that act as exit points for emigrating neutrophils. *J. Exp. Med.* **203**, 1519–1532 (2006).
- Reese, T.S. & Karnovsky, M.J. Fine structural localization of a blood-brain barrier to exogenous peroxidase. *J. Cell Biol.* **34**, 207–217 (1967).
- Toft-Hansen, H. *et al.* Metalloproteinases control brain inflammation induced by pertussis toxin in mice overexpressing the chemokine CCL2 in the central nervous system. *J. Immunol.* **177**, 7242–7249 (2006).
- Kerfoot, S.M. & Kubers, P. Overlapping roles of P-selectin and α₄ integrin to recruit leukocytes to the central nervous system in experimental autoimmune encephalomyelitis. *J. Immunol.* **169**, 1000–1006 (2002).
- Vajkoczy, P., Laschinger, M. & Engelhardt, B. α₄-integrin–VCAM-1 binding mediates G protein–independent capture of encephalitogenic T cell blasts to CNS white matter microvessels. *J. Clin. Invest.* **108**, 557–565 (2001).
- Engelhardt, B. Molecular mechanisms involved in T cell migration across the blood-brain barrier. *J. Neural Transm.* **113**, 477–485 (2006).
- Alt, C., Laschinger, M. & Engelhardt, B. Functional expression of the lymphoid chemokines CCL19 (ELC) and CCL 21 (SLC) at the blood-brain barrier suggests their involvement in G-protein–dependent lymphocyte recruitment into the central nervous system during experimental autoimmune encephalomyelitis. *Eur. J. Immunol.* **32**, 2133–2144 (2002).
- Babcock, A.A., Kuziel, W.A., Rivest, S. & Owens, T. Chemokine expression by glial cells directs leukocytes to sites of axonal injury in the CNS. *J. Neurosci.* **23**, 7922–7930 (2003).
- Glabinski, A.R., Tani, M., Tuohy, V.K., Tuthill, R.J. & Ransohoff, R.M. Central nervous system chemokine mRNA accumulation follows initial leukocyte entry at the onset of acute murine experimental autoimmune encephalomyelitis. *Brain Behav. Immun.* **9**, 315–330 (1995).
- Geberhiwot, T. *et al.* Laminin-8 (α4β1γ1) is synthesized by lymphoid cells, promotes lymphocyte migration and costimulates T cell proliferation. *J. Cell Sci.* **114**, 423–433 (2001).
- Gorfu, G. *et al.* Laminin isoforms of lymph nodes and predominant role of α5-laminin(s) in adhesion and migration of blood lymphocytes. *J. Leukoc. Biol.* **84**, 701–712 (2008).
- Thyboll, J. *et al.* Deletion of the laminin α4 chain leads to impaired microvessel maturation. *Mol. Cell. Biol.* **22**, 1194–1202 (2002).
- Frieser, M. *et al.* Cloning of the mouse laminin α4 gene: expression in a subset of endothelium. *Eur. J. Biochem.* **246**, 727–735 (1997).
- Bai, X.F. *et al.* CD24 controls expansion and persistence of autoreactive T cells in the central nervous system during experimental autoimmune encephalomyelitis. *J. Exp. Med.* **200**, 447–458 (2004).
- Flügel, A. *et al.* Migratory activity and functional changes of green fluorescent effector cells before and during experimental autoimmune encephalomyelitis. *Immunity* **14**, 547–560 (2001).

25. Gimond, C. *et al.* Cre-*loxP*-mediated inactivation of the α_{6A} integrin spliced variant *in vivo*: evidence for a specific functional role of α_{6A} in lymphocyte migration but not in heart development. *J. Cell Biol.* **143**, 253–266 (1998).
26. Georges-Labouesse, E. *et al.* Absence of integrin α_6 leads to epidermolysis bullosa and neonatal death in mice. *Nat. Genet.* **13**, 370–373 (1996).
27. Thompson, R.D. *et al.* Platelet-endothelial cell adhesion molecule-1 (PECAM-1)-deficient mice demonstrate a transient and cytokine-specific role for PECAM-1 in leukocyte migration through the perivascular basement membrane. *Blood* **97**, 1854–1860 (2001).
28. Wakelin, M.W. *et al.* An anti-platelet-endothelial cell adhesion molecule-1 antibody inhibits leukocyte extravasation from mesenteric microvessels *in vivo* by blocking the passage through the basement membrane. *J. Exp. Med.* **184**, 229–239 (1996).
29. Patton, B.L. *et al.* Properly formed but improperly localized synaptic specializations in the absence of laminin $\alpha 4$. *Nat. Neurosci.* **4**, 597–604 (2001).
30. Wang, J. *et al.* Cardiomyopathy associated with microcirculation dysfunction in laminin $\alpha 4$ chain-deficient mice. *J. Biol. Chem.* **281**, 213–220 (2006).
31. Colognato, H. & Yurchenco, P.D. Form and function: the laminin family of heterotrimers. *Dev. Dyn.* **218**, 213–234 (2000).
32. Yurchenco, P.D., Smirnov, S. & Mathus, T. Analysis of basement membrane self-assembly and cellular interactions with native and recombinant glycoproteins. *Methods Cell Biol.* **69**, 111–144 (2002).
33. Galea, I. *et al.* An antigen-specific pathway for CD8 T cells across the blood-brain barrier. *J. Exp. Med.* **204**, 2023–2030 (2007).
34. Fujiwara, H., Kikkawa, Y., Sanzen, N. & Sekiguchi, K. Purification and characterization of human laminin-8. Laminin-8 stimulates cell adhesion and migration through $\alpha_3\beta_1$ and $\alpha_6\beta_1$ integrins. *J. Biol. Chem.* **276**, 17550–17558 (2001).
35. Fujiwara, H., Gu, J. & Sekiguchi, K. Rac regulates integrin-mediated endothelial cell adhesion and migration on laminin-8. *Exp. Cell Res.* **292**, 67–77 (2004).
36. Greter, M. *et al.* Dendritic cells permit immune invasion of the CNS in an animal model of multiple sclerosis. *Nat. Med.* **11**, 328–334 (2005).
37. Engelhardt, B. The blood-central nervous system barriers actively control immune cell entry into the central nervous system. *Curr. Pharm. Des.* **14**, 1555–1565 (2008).
38. Nasdala, I. *et al.* A transmembrane tight junction protein selectively expressed on endothelial cells and platelets. *J. Biol. Chem.* **277**, 16294–16303 (2002).
39. Rehder, D. *et al.* Junctional adhesion molecule-a participates in the formation of apico-basal polarity through different domains. *Exp. Cell Res.* **312**, 3389–3403 (2006).
40. Sorokin, L.M. *et al.* Developmental regulation of laminin $\alpha 5$ suggests a role in epithelial and endothelial cell maturation. *Dev. Biol.* **189**, 285–300 (1997).
41. Ford, A.L., Goodsall, A., Hickey, W. & Sedgwick, J. Normal adult ramified microglia separated from other CNS macrophages by flow cytometric sorting. *J. Immunol.* **154**, 4309–4321 (1995).
42. Sixt, M., Hallmann, R., Wendler, O., Scharffetter-Kochanek, K. & Sorokin, L.M. Cell adhesion and migration properties of β_2 -integrin negative, polymorphonuclear granulocytes (PMN) on defined extracellular matrix molecules: relevance for leukocyte extravasation. *J. Biol. Chem.* **276**, 18878–18887 (2001).